

Suppression of Diacylglycerol Acyltransferase-2 (*DGAT2*), but Not *DGAT1*, with Antisense Oligonucleotides Reverses Diet-induced Hepatic Steatosis and Insulin Resistance^{*[5]}

Received for publication, May 22, 2007 Published, JBC Papers in Press, May 27, 2007, DOI 10.1074/jbc.M704213200

Cheol Soo Choi^{†1}, David B. Savage^{†1,2}, Ameya Kulkarni^{†1}, Xing Xian Yu^{§3}, Zhen-Xiang Liu[‡], Katsutaro Morino[‡], Sheene Kim[‡], Alberto Distefano[‡], Varman T. Samuel[‡], Susanne Neschen[‡], Dongyan Zhang[‡], Amy Wang[‡], Xian-Man Zhang[‡], Mario Kahn[‡], Gary W. Cline[‡], Sanjay K. Pandey[§], John G. Geisler[§], Sanjay Bhanot^{§3}, Brett P. Monia^{§3}, and Gerald I. Shulman^{†¶4}

From the Departments of [†]Internal Medicine and [¶]Cellular and Molecular Physiology, ^{||}Howard Hughes Medical Institute, Yale University School of Medicine, New Haven, Connecticut 06510 and [§]Isis Pharmaceuticals, Carlsbad, California 92008

Nonalcoholic fatty liver disease (NAFLD) is a major contributing factor to hepatic insulin resistance in type 2 diabetes. Diacylglycerol acyltransferase (*Dgat*), of which there are two isoforms (*Dgat1* and *Dgat2*), catalyzes the final step in triglyceride synthesis. We evaluated the metabolic impact of pharmacological reduction of *DGAT1* and *-2* expression in liver and fat using antisense oligonucleotides (ASOs) in rats with diet-induced NAFLD. *Dgat1* and *Dgat2* ASO treatment selectively reduced *DGAT1* and *DGAT2* mRNA levels in liver and fat, but only *Dgat2* ASO treatment significantly reduced hepatic lipids (diacylglycerol and triglyceride but not long chain acyl CoAs) and improved hepatic insulin sensitivity. Because *Dgat* catalyzes triglyceride synthesis from diacylglycerol, and because we have hypothesized that diacylglycerol accumulation triggers fat-induced hepatic insulin resistance through protein kinase C ϵ activation, we next sought to understand the paradoxical reduction in diacylglycerol in *Dgat2* ASO-treated rats. Within 3 days of starting *Dgat2* ASO therapy in high fat-fed rats, plasma fatty acids increased, whereas hepatic lysophosphatidic acid and diacylglycerol levels were similar to those of control rats. These changes were associated with reduced expression of lipogenic genes (*SREBP1c*, *ACCL1*, *SCD1*, and *mtGPAT*) and increased expression of oxidative/thermogenic genes (*CPT1* and *UCP2*). Taken together, these data suggest that knocking down *Dgat2* protects against fat-induced hepatic insulin resistance by paradoxically lowering hepatic diacylglycerol content and protein kinase C ϵ activation through decreased *SREBP1c*-mediated lipogenesis and increased hepatic fatty acid oxidation.

Nonalcoholic fatty liver disease (NAFLD)⁵ is the most frequent cause of abnormal liver function tests in the United States (estimated prevalence of 14–20%) (1, 2). It is caused by triglyceride (TG) accumulation within the liver and is strongly associated with insulin resistance, type 2 diabetes mellitus (T2DM), and the metabolic syndrome (3, 4). Accumulating evidence suggests that hepatic lipid accumulation causes hepatic insulin resistance. For example, increasing hepatic lipid stores in mice by overexpressing lipoprotein lipase in the liver (5) and in rats by short term high fat feeding (6) results in liver-specific fat accumulation and hepatic insulin resistance. Several strategies have been employed to reduce hepatic steatosis in rodents; these include treatment with a mitochondrial uncoupling agent (2,4-dinitrophenol) (6), antisense oligonucleotide inhibition of acetyl-coenzyme A carboxylase I and II (7), adenoviral overexpression of malonyl-CoA decarboxylase (8), and transgenic overexpression of uncoupling protein 1 (9), all of which successfully ameliorated hepatic insulin resistance. We have also shown that moderate weight loss in patients with T2DM lowers liver triglycerides and specifically improves hepatic insulin sensitivity (10). Although the above data strongly suggest that hepatic lipid accumulation causes hepatic insulin resistance, the molecular mechanisms responsible for this relationship remain uncertain. We have proposed a model in which excess diacylglycerol (DAG) activates protein kinase C ϵ (PKC ϵ), a serine/threonine kinase that in turn binds to the insulin receptor and inhibits its tyrosine kinase activity (11). Until very recently, long chain acyl-coenzymes A (LCCoAs) were a favored candidate for fat-induced insulin resistance, but recent studies in mitochondrial acyl-coenzyme A (CoA):glycerol-*sn*-3-phosphate acyltransferase (*mtGPAT*) knock-out mice, which accumulate LCCoAs in the liver but have reduced liver DAG con-

^{*} This work was supported in part by United States Public Health Service Grants R01 DK-40936 (to G. I. S.) and P30 DK-45735 (to G. I. S.) and a Distinguished Clinical Scientist Award from the American Diabetes Association. The costs of publication of this article were defrayed in part by the payment of page charges. This article must therefore be hereby marked "advertisement" in accordance with 18 U.S.C. Section 1734 solely to indicate this fact.

[5] The on-line version of this article (available at <http://www.jbc.org>) contains supplemental Table 1.

¹ These authors contributed equally to this work.

² Supported by the Wellcome Trust.

³ Employee of and owns stock and/or holds stock options in Isis Pharmaceuticals.

⁴ Investigator of the Howard Hughes Medical Institute. To whom correspondence should be addressed: TAC S269 P. O. Box 9812, Yale University School of Medicine, New Haven, CT 06536-9812. Tel.: 203-785-5447; Fax: 203-737-4059; E-mail: gerald.shulman@yale.edu.

⁵ The abbreviations used are: NAFLD, nonalcoholic fatty liver disease; ASOs, antisense oligonucleotides; ASOctrl, ASO control; CPT1, carnitine palmitoyltransferase 1; CoA, coenzyme A; DAG, diacylglycerol; DGAT, acyl-CoA: diacylglycerol acyltransferase; FFA, free fatty acid; HFD, high fat diet; LCCoA, long chain acyl CoA; LPA, lysophosphatidic acid; mtGPAT, mitochondrial acyl-CoA:glycerol-*sn*-3-phosphate acyltransferase; PPAR α , peroxisome proliferator-activated receptor α ; PKC, protein kinase C; PUFAs, polyunsaturated fatty acids; SCD1, stearoyl-CoA desaturase 1; SREBP1c, sterol-regulatory element-binding protein 1c; TG, triglyceride; T2DM, type 2 diabetes mellitus; RT, reverse transcription; HPLC, high pressure liquid chromatography; 2-DG-6-P, 2-[¹⁴C]deoxyglucose 6-phosphate; PI3K, phosphatidylinositol 3-kinase.

tent and are protected from fat-induced hepatic insulin resistance (12), suggested that DAG may be a better candidate. DAG is also a potent activator of novel PKCs (13–15), making it an excellent candidate for this role.

Acyl-CoA:diacylglycerol acyltransferase (Dgat) catalyzes the final step in TG synthesis by facilitating the linkage of *sn*-1,2-diacylglycerol (DAG) with an LCCoA. Dgat exists in two primary isoforms: Dgat1 and Dgat2 (16, 17); Dgat1 is most highly expressed in small intestine and white adipose tissue, whereas Dgat2 is primarily expressed in liver and white adipose tissue (16, 17) where its expression is insulin-responsive. There is some evidence suggesting that the two enzymes play different roles in TG metabolism. *DGAT1* knock-out mice have ~50% less TG in tissues and are protected from diet-induced obesity and insulin resistance through a mechanism involving increased energy expenditure (at least partly attributable to increased physical activity) (18, 19). Study of Dgat2 has been more difficult as homozygous *DGAT2* knock-out mice die shortly after birth because of severe lipopenia (~90% TG reduction in *DGAT2* null carcasses) and impaired skin barrier function (20).

Here we sought to address two key questions. First, what effect does *DGAT1* or *DGAT2* knockdown in liver and fat have on hepatic insulin action? Other than the *mtGPAT* knock-out model, previous successful therapeutic strategies for NAFLD have primarily focused on increasing fat oxidation as opposed to inhibiting fat synthesis. In this study, we were therefore interested in examining the effect of inhibiting another key regulator of fat synthesis. Second, which lipid intermediates are increased or decreased by *DGAT* knockdown? Conventional wisdom suggests that DAG, a substrate for the enzyme activity of Dgat, might accumulate in the face of Dgat knockdown, an event which we have suggested induces insulin resistance (21–23). The present study demonstrates that Dgat2, but not Dgat1 ASO treatment, improves hepatic steatosis, insulin sensitivity, and somewhat surprisingly reduces hepatic DAG content. In addition, we provide evidence suggesting a potential mechanism to explain this paradoxical effect of *DGAT2* inhibition on hepatic DAG content.

EXPERIMENTAL PROCEDURES

Animals—All rats were maintained in accordance with the Institutional Animal Care and Use Committee of Yale University School of Medicine. Healthy male Sprague-Dawley rats weighing ~200 g were obtained from Charles River Laboratories and acclimated for 1 week after arrival before initiation of the experiment. Rats received food and water *ad libitum* and were maintained on a 12:12 h light/dark cycle (lights on at 6:30 a.m.). They were housed individually, and food consumption and body weight were monitored. Rats received either regular rodent chow (60% carbohydrate, 10% fat, 30% protein calories) or a high fat diet (26% carbohydrate, 59% fat, 15% protein calories). Safflower oil was the major constituent of the high fat diet (Dyets Inc.). We have shown previously that this diet produces hepatic steatosis and hepatic insulin resistance within 3 days (6). Intraperitoneal ASO therapy was initiated 3 days after commencing the high fat diet. All ASOs (control, Dgat1, and Dgat2) were prepared in normal saline, and the solutions were steril-

ized through a 0.2- μ m filter. Rats were given ASO solutions or saline twice per week via intraperitoneal injection at a dose of 50 or 75 mg/kg/week for 4 weeks. ASO control rats were treated at the higher dose (75 mg/kg/week). During the treatment period, body weight and food intake were measured twice weekly. The Yale Animal Care and Use Committee approved all protocols.

Selection of Rat Dgat ASOs—To identify rat Dgat1 and Dgat2 ASO inhibitors, rapid throughput screens were performed *in vitro* as described previously (24). In brief, 80 ASOs were designed to the rat *DGAT1* and *DGAT2* mRNAs sequences, respectively, and initial screens identified several potent and specific ASOs, all of which targeted a binding site within the coding region of the *DGAT1* and *DGAT2* mRNAs. After extensive dose-response characterization of the most potent ASOs from the screen, two lead ASOs, ISIS-327822 (sequence CCT-TCGCTGGCGGCACCACA) for Dgat1 and ISIS-369235 (sequence GCATTACCACTCCCATTCTT) for Dgat2, were chosen. The control ASO, ISIS-141923, has the following sequence, 5'-CCTTCCCTGAAGGTTCCCTCC-3', and does not have perfect complementarity to any known gene in public data bases. The first five bases and last five bases of chimeric ASOs have a 2'-*O*-(2-methoxy)-ethyl modification, and the ASOs also have a phosphorothioate backbone. This chimeric design has been shown to provide both increased nuclease resistance and mRNA affinity, while maintaining the robust RNase H terminating mechanism utilized by these types of ASOs (25). These benefits result in an attractive *in vivo* pharmacological and toxicological profile for 2'-*O*-(2-methoxy)-ethyl chimeric ASOs.

Determination of DGAT Activity in Liver Homogenates and Fatty Acid Oxidation and Triglyceride Synthesis in Transfected Rat Hepatocytes in Vitro—Total DGAT activity was measured in liver tissue homogenates from ASO-treated rats as described previously (16, 26). Primary rat hepatocytes were isolated as described previously and plated onto collagen-coated 25-cm² flasks for fatty acid oxidation measurement or 60-mm plates for triglyceride synthesis measurement (27). Hepatocytes were treated with ASO (150 nM) and Lipofectin® (Invitrogen) mixture for 4 h in serum-free William's E media (Invitrogen). ASO and Lipofectin were mixed in a ratio of 3 μ g of Lipofectin® for every 1 ml of 100 nM ASO concentration. After 4 h, ASO reaction mixture was replaced with normal maintenance media (William's E media with 10% fetal bovine serum and 10 nM insulin). The cells were incubated under normal conditions for 20–24 h, and then fatty acid ([¹⁴C]oleate) oxidation and triglyceride synthesis (incorporation of [³H]glycerol into triglyceride) were measured as described previously (27).

Hyperinsulinemic-Euglycemic Clamp Studies—Seven days prior to the hyperinsulinemic-euglycemic clamp studies, indwelling catheters were placed into the right internal jugular vein extending to the right atrium, and the left carotid artery extending to the aortic arch. After an overnight fast, [3-³H]glucose (HPLC-purified; PerkinElmer Life Sciences) was infused at a rate of 0.15 μ Ci/min for 3 h to assess the basal glucose turnover. Following the basal period, the hyperinsulinemic-euglycemic clamp was conducted for 135 min with a primed/continuous infusion of human insulin (60 milliunits/kg prime, 4 milliunits/kg/min infusion) (Novo Nordisk) and a variable infusion of 20%

Suppressing DGAT2 Reverses Hepatic Insulin Resistance

dextrose to maintain euglycemia (~ 100 mg/dl). [$3\text{-}^3\text{H}$]Glucose was infused at a rate of $0.4 \mu\text{Ci}/\text{min}$ throughout the clamps. A $25\text{-}\mu\text{Ci}$ bolus of 2-deoxy-D-[$1\text{-}^{14}\text{C}$]glucose (PerkinElmer Life Sciences) was injected at the 90th min of the clamp to estimate the rate of insulin-stimulated tissue glucose uptake. Additional blood samples ($20\text{--}60 \mu\text{l}$) were taken at 0, 70, and 135 min for the determination of plasma FFA and/or insulin concentrations. At the end of the clamp, rats were anesthetized with pentobarbital sodium injection ($150 \text{ mg}/\text{kg}$), and all tissues were taken within 4 min, frozen immediately using liquid N_2 -cooled aluminum tongs, and stored at -80°C for subsequent analysis.

Biochemical Analysis and Calculations—Plasma glucose was analyzed during the clamps using $10 \mu\text{l}$ of plasma by a glucose oxidase method on a Beckman glucose analyzer II (Beckman Coulter). Plasma insulin, adiponectin, and leptin were measured by radioimmunoassay using kits from Linco Research Inc. The adiponectin kit was primarily designed to measure mouse adiponectin, but it shows significant cross-reactivity with rat adiponectin. Plasma fatty acid concentrations were determined using an acyl-CoA oxidase-based colorimetric kit (Wako Pure Chemical Industries Ltd.). Plasma lipoprotein and cholesterol profiling in pooled samples of each group was performed with a Beckman System Gold 126 HPLC system, 507e refrigerated autosampler, 126-photodiode array detector (Beckman Instruments, Fullerton, CA) and a Superose 6 HR 10/30 column (Pfizer, Chicago) as described by Crooke *et al.* (28). For the determination of plasma [^3H]glucose, plasma was deproteinized with ZnSO_4 and $\text{Ba}(\text{OH})_2$, dried to remove $^3\text{H}_2\text{O}$, resuspended in water, and counted in scintillation fluid (Ultima Gold, PerkinElmer Life Sciences) on a Beckman scintillation counter. Rates of basal and insulin-stimulated whole body glucose turnover were determined as the ratio of the [$3\text{-}^3\text{H}$]glucose infusion rate (disintegrations per min (dpm)) to the specific activity of plasma glucose (dpm per mg) at the end of the basal period and during the final 30 min of the clamp experiment, respectively. Hepatic glucose production was determined by subtracting the glucose infusion rate from the rate of total glucose appearance. The plasma concentration of $^3\text{H}_2\text{O}$ was determined by the difference between ^3H counts without and with drying, and whole body glycolysis was calculated from the rate of increase in plasma $^3\text{H}_2\text{O}$ concentration, determined by linear regression of the measurements at 100, 105, 115, 125, and 135 min (29). Whole body glycogen synthesis was estimated by subtracting whole body glycolysis from whole body glucose uptake, assuming that glycolysis and glycogen synthesis account for the majority of insulin-stimulated glucose uptake (30). Glucose uptake and glycogen synthesis in individual muscles were calculated from muscle 2-[^{14}C]deoxyglucose 6-phosphate (2-DG-6-P) content and ^3H incorporation into muscle glycogen as described previously (29). For the determination of muscle 2-DG-6-P content, muscle samples were homogenized, and the supernatants were subjected to an ion-exchange column to separate 2-DG-6-P from 2-DG as described previously (31). The radioactivity of ^3H in muscle glycogen was determined by digesting muscle samples in KOH and precipitating glycogen with EtOH as described previously (30).

Tissue Lipid Measurement—The solid-phase extraction and purification of medium, long chain, and very long chain fatty

acyl-CoAs from liver have been described previously (32, 33). After purification, fatty acyl-CoA fractions were dissolved in methanol/ H_2O (1:1, v/v) and subjected to lipid chromatography/tandem mass spectrometry analysis. A turbo ion spray source was interfaced with an API 3000 tandem mass spectrometer (Applied Biosystems) in conjunction with two 200 series micro pumps and a 200 series autosampler (PerkinElmer Life Sciences). The DAG extraction and analysis were performed as described previously (12, 15). Total DAG content is expressed as the sum of individual species. Tissue TG was extracted using the method of Bligh and Dyer (32) and measured using a DCL triglyceride reagent (Diagnostic Chemicals Ltd.). Tissue lysophosphatidic acid (LPA) content was measured as described previously (12). In short, ~ 100 mg of liver tissue was homogenized in chloroform/methanol (1:1 v/v) with 1 nmol of C17-lysophosphatidic acid as an internal standard. After phase separation with H_2O , samples were vortexed and centrifuged, and the methanol/water phase was collected. The supernatant was applied to conditioned Waters Oasis HLB extraction cartridges (Waters), and after a washing step LPA was eluted using methanol. Individual LPA derivatives were measured using lipid chromatography/tandem mass spectrometry analysis, and total LPA content was expressed as the sum of individual species.

Insulin Signaling—IRS2-associated PI3K and Akt2 activity were assessed in protein extracts from livers harvested after short term insulin stimulation. PI3K and Akt2 assays were performed according to methods previously described (6, 34–36). Primary antibodies used for experiments were rabbit polyclonal IgG. Antibodies for PI3K and Akt2 were obtained from Upstate (Charlottesville, VA).

For PKC ϵ membrane translocation, $50 \mu\text{g}$ of crude membrane and cytosol protein extracts were resolved by SDS-PAGE using 8% gel and electroblotted onto polyvinylidene difluoride membrane (DuPont) using a semidry-transfer cell (Bio-Rad). The membrane was then blocked for 2 h at room temperature in phosphate-buffered saline/Tween (PBS-T:10 mmol/liter NaH_2PO_4 , 80 mmol/liter Na_2HPO_4 , 0.145 mol/liter NaCl, and 0.1% Tween 20, pH 7.4) containing 5% (w/v) nonfat dried milk, washed twice, and then incubated overnight with rabbit anti-peptide antibody against PKC ϵ (Santa Cruz Biotechnology) diluted 1:100 in rinsing solution. After further washings, membranes were incubated with horseradish peroxidase-conjugated IgG fraction of goat anti-rabbit IgG (Bio-Rad), diluted 1:5000 in PBS-T, for 2 h. PKC ϵ translocation was expressed as the ratio of membrane bands over cytosol bands (arbitrary units).

Total RNA Preparation, Real Time Quantitative RT-PCR Analysis, and Immunoblotting Analysis—Total RNA was extracted using total RNA isolation reagent (BL-10500, Biotecx Laboratories Inc.) according to manufacturer's instructions. Real time quantitative RT-PCR was performed using custom-made RT-PCR enzymes and reagents kit (Invitrogen) and ABI Prism 7700 sequence detector (Applied Biosciences). Primers and probes for analysis of the expression of different genes (supplemental Table 1) were designed using Primer Express Software (Applied Biosciences). For the analysis, 100 ng of total RNA was used. Each RNA sample was run in duplicate, and the

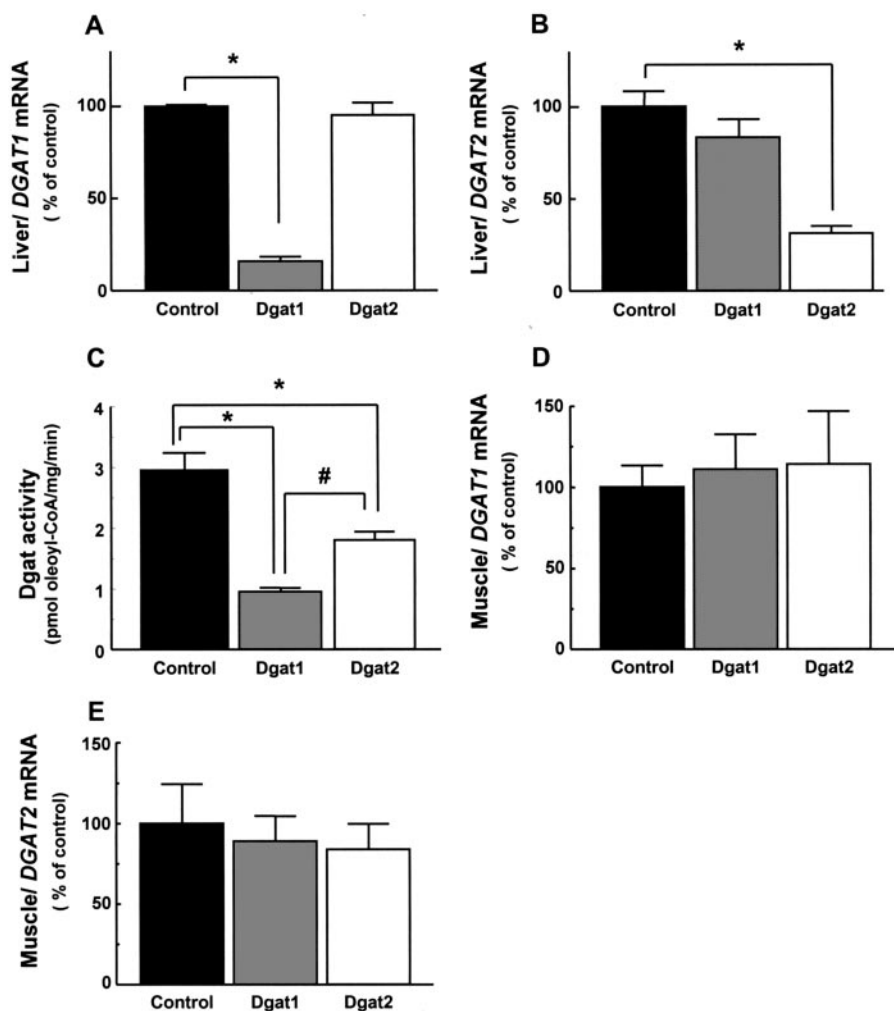


FIGURE 1. Dgat ASOs selectively decrease DGAT expression in high fat-fed rat liver. After 4 weeks of ASO treatment, total RNA was isolated from liver (A and B) and muscle (D and E), and gene expression (*DGAT1* mRNA (A and D) and *DGAT2* mRNA (B and E)) was then assessed by real time RT-PCR. Total Dgat activity was also measured in liver tissue homogenates from liver (C). All data are expressed as mean values \pm S.E. of six rats per treatment group, and error bars indicate S.E. *, $p < 0.05$ versus ASOctrl; #, $p < 0.05$ versus Dgat1 ASO treatment group.

mean value was used to calculate the gene expression level. For Western protein analysis, 200 μ l of homogenization buffer (160 NaCl, 20 Trizma (Tris base), 1 EDTA, 1 EGTA, 1 dithiothreitol, 1% Triton X-100, 0.1% SDS, 1 sodium orthovanadate, 1 sodium fluoride, 1 phenylmethylsulfonyl fluoride, 0.5 μ g/ml leupeptin, and 0.5 μ g/ml pepstatin A) was added to 20 mg of powdered tissue. After homogenization for 15 min on ice, the samples were transferred to microcentrifuge tubes and rotated on a rocking platform for 30 min in the cold room. After centrifugation for 60 min at 20,500 relative centrifugal fields in a refrigerated centrifuge at 4 $^{\circ}$ C, insoluble debris was removed. Forty micrograms of tissue lysates were then separated on 4–12% SDS-PAGE and immunoblotted with SREBP1 (Santa Cruz Biotechnology, catalog number 13551), ACC1 (Cell Signaling, catalog number 36620), SCD1 (Santa Cruz Biotechnology, catalog number 14720), or UCP2 (Santa Cruz Biotechnology, catalog number 6526) antibodies.

Fat Absorption—During the treatment period, fat absorption was measured by placing a sucrose polybehenate marker in a

safflower oil diet and measuring the percent discarded in collected stool samples (37).

Statistical Analysis—Data are expressed as means \pm S.E. The significance of the differences in mean values among the three groups was evaluated using the one-way analysis of variance, followed by *ad hoc* analysis using the (Duncan's test). Statistical analyses for the two groups were made using a two-tailed Student's *t* test, and $p < 0.05$ was considered statistically significant.

RESULTS

Dgat ASOs Reduce DGAT Expression—After 3 days on a high fat diet, an interval that allows for significant fat accumulation in the liver (6), rats were treated with control (ASOctrl), Dgat1, or Dgat2 ASOs at 25 (for Dgat1) or 37.5 (for Dgat2 and ASOctrl) mg per kg body weight twice a week for 4 weeks. In comparison with ASOctrl, Dgat1 and Dgat2 ASO treatment selectively reduced *DGAT1* (Fig. 1A) and *DGAT2* mRNA (Fig. 1B) levels by ~84 and 70%, respectively, in the liver. Both ASOs significantly reduced total Dgat activity in liver homogenates (Fig. 1C). Dgat1 ASO had a greater effect on total Dgat activity than Dgat2 ASO because assay conditions for total Dgat activity with 20 mM MgCl₂ are optimized for DGAT1 rather than

DGAT2 activity (16, 17). To exclude off-target effects of Dgat2 ASO, mRNA expression of acyl-coenzyme A:monoacylglycerol acyltransferase (Mgat) 1, 2, and 3 were tested in liver because they catalyze the synthesis of DAG from monoacylglycerol and share sequence homology with *DGAT2* (38–41). In addition, they have some Dgat activity (38–41). *MGAT1* mRNA expression is unaltered in the liver (ASOctrl versus Dgat2 ASO; 0.09 ± 0.01 versus 0.11 ± 0.02 arbitrary units, not significant). *MGAT2* is expressed at very low levels in rat liver (barely detectable using RT-PCR), and *MGAT3* is suggested to be specific to the intestine in rodents (40). Target gene expression was reduced to a similar extent in adipose tissue (90 and 87% for *DGAT1* and *DGAT2*, respectively), but no significant changes were seen in *DGAT* expression in muscle (Fig. 1, D and E). There was no compensatory increase in the untargeted isoform. None of the ASOs appeared to be associated with overt toxicity as assessed by hepatic transaminase levels (Table 1) and food intake.

Suppressing DGAT2 Reverses Hepatic Insulin Resistance

TABLE 1

Metabolic parameters during fasting and hyperinsulinemic-euglycemic clamp periods

Fasting refers to an overnight fast.

Group	Control		Dgat1		Dgat2	
	Fasting (<i>n</i> = 8)	Clamp (<i>n</i> = 11)	Fasting (<i>n</i> = 7)	Clamp (<i>n</i> = 11)	Fasting (<i>n</i> = 7)	Clamp (<i>n</i> = 9)
Body weight (g)	422 ± 7	401 ± 8	415 ± 11	412 ± 11	407 ± 13	370 ± 8 ^a
Epididymal fat mass (g)	5.9 ± 1.0	ND	ND	ND	2.9 ± 0.4 ^b	ND
Glucose (mg/dl)	116 ± 3.0	111 ± 2.5	125 ± 3.0	98.5 ± 2.2	125 ± 6.7	114 ± 2.7
Insulin (microunits/liter)	7.3 ± 1.6	96.1 ± 7.0	13.6 ± 5.4	99.1 ± 7.7	3.4 ± 0.7 ^c	97.7 ± 4.8
FA (meq/liter)	0.84 ± 0.06	0.43 ± 0.03	0.82 ± 0.08	0.49 ± 0.06	0.64 ± 0.05	0.23 ± 0.04 ^d
Plasma TG (mg/dl)	36.0 ± 2.2	ND	34.9 ± 1.7	ND	26.1 ± 1.3 ^c	ND
Plasma cholesterol (mg/dl)	40.3 ± 2.2	ND	50.1 ± 6.2	ND	32.7 ± 2.3 ^c	ND
Leptin (ng/ml)	2.2 ± 0.3	ND	3.2 ± 0.46	ND	1.23 ± 0.27 ^c	ND
Adiponectin (μg/ml)	3.2 ± 0.4	ND	ND	ND	2.6 ± 0.36	ND
ALT (units/liter) ^d	38 ± 2.5	ND	41 ± 3.0	ND	42 ± 1.7	ND

^a*p* < 0.05 Dgat2 (clamp) versus control and Dgat1 (clamp).

^b*p* < 0.05 Dgat2 (fasting) versus control (fasting).

^c*p* < 0.05 Dgat2 (fasting) versus control and Dgat1 (fasting).

^dALT is alanine aminotransferase; ND is not determined.

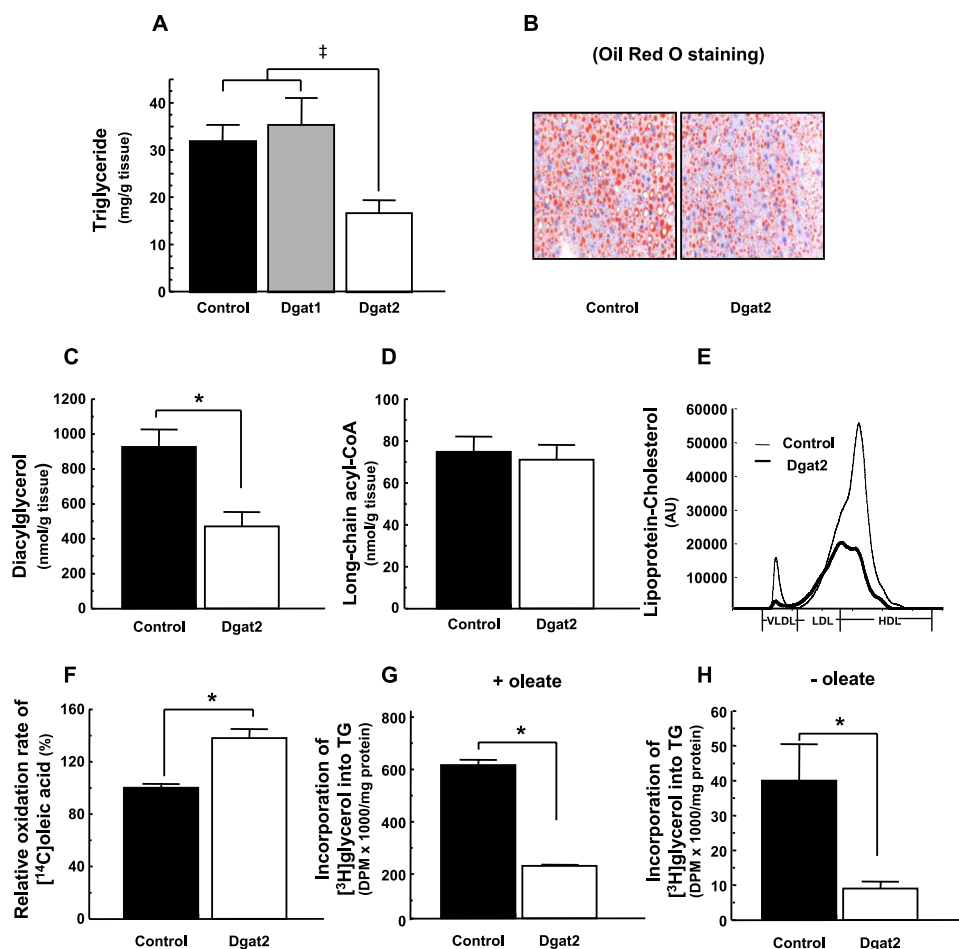


FIGURE 2. Dgat2 ASO lowers hepatic lipid levels by increasing fat oxidation and reducing fat synthesis in high fat fed rats. TG (A), DAG (C), and LCCoA levels (D) were observed in rat livers after 4 weeks of ASO therapy. B, Oil red O staining of liver from control and Dgat2 ASO-treated rats. Plasma lipoprotein and cholesterol profile were measured from pooled samples of each group (E). Fatty acid oxidation (F) and triglyceride (TG) synthesis (G and H) were measured in primary rat hepatocytes. Data are expressed as mean values ± S.E. of 7–8 rats per treatment group or *n* = 3 experiments in isolated hepatocytes; error bars indicate S.E. †, *p* < 0.05 versus ASOctrl and Dgat1 ASO; *, *p* < 0.05 versus ASOctrl treatment group.

Food Intake and Body Weight Response—Dgat2 ASO therapy was associated with a small decrease in body weight and epididymal fat pad mass (Table 1). As caloric intake (ASOctrl versus Dgat2 ASO; 98.8 ± 2.3 versus 97.0 ± 8.2 kcal/day) and intestinal fat absorption (ASOctrl versus Dgat2; 99.1 ± 0.4% versus 99.4 ±

0.4%) were similar in control and Dgat2 treated rats, these data suggest that energy expenditure was slightly increased in the Dgat2 ASO treatment group.

Dgat2 ASO Reduces Liver and Muscle Steatosis and Plasma Triglycerides—Hepatic TGs were markedly reduced by Dgat2 ASO (50% reduction, *p* < 0.05) but not by Dgat1 ASO treatment (Fig. 2, A and B). DAG levels were also substantially decreased by 4 weeks of Dgat2 ASO therapy (53% reduction, *p* < 0.05) (Fig. 2C), whereas LCCoAs were unchanged (Fig. 2D). Fasting plasma TGs and total cholesterol fell by 28 and 19%, respectively, in the Dgat2 ASO group, whereas plasma fatty acids were unchanged in fasting rats after 4 weeks of treatment (Table 1). Very low density lipoprotein and high density lipoprotein cholesterol were both substantially reduced in Dgat2 ASO-treated rats (Fig. 2E). *In vitro* studies in primary rat hepatocytes suggest that reduced TG synthesis is likely to be the primary mechanism for the observed reduction in liver lipids (Fig. 2, F–H), although fat oxidation was also significantly increased. In addition, muscle TG content was reduced by 33% in the Dgat2 ASO group (ASOctrl versus Dgat2; 5.67 ± 0.51 versus 3.80 ± 0.69 mg/g tissue, *p* < 0.05).

Dgat2 ASO Treatment Improves Hepatic Insulin Sensitivity—Fasting plasma glucose and fatty acid concentrations were similar in both groups after 4 weeks of ASO therapy, whereas plasma insulin concentrations were significantly reduced in Dgat2 ASO-treated rats (Table 1). Leptin levels were also lower

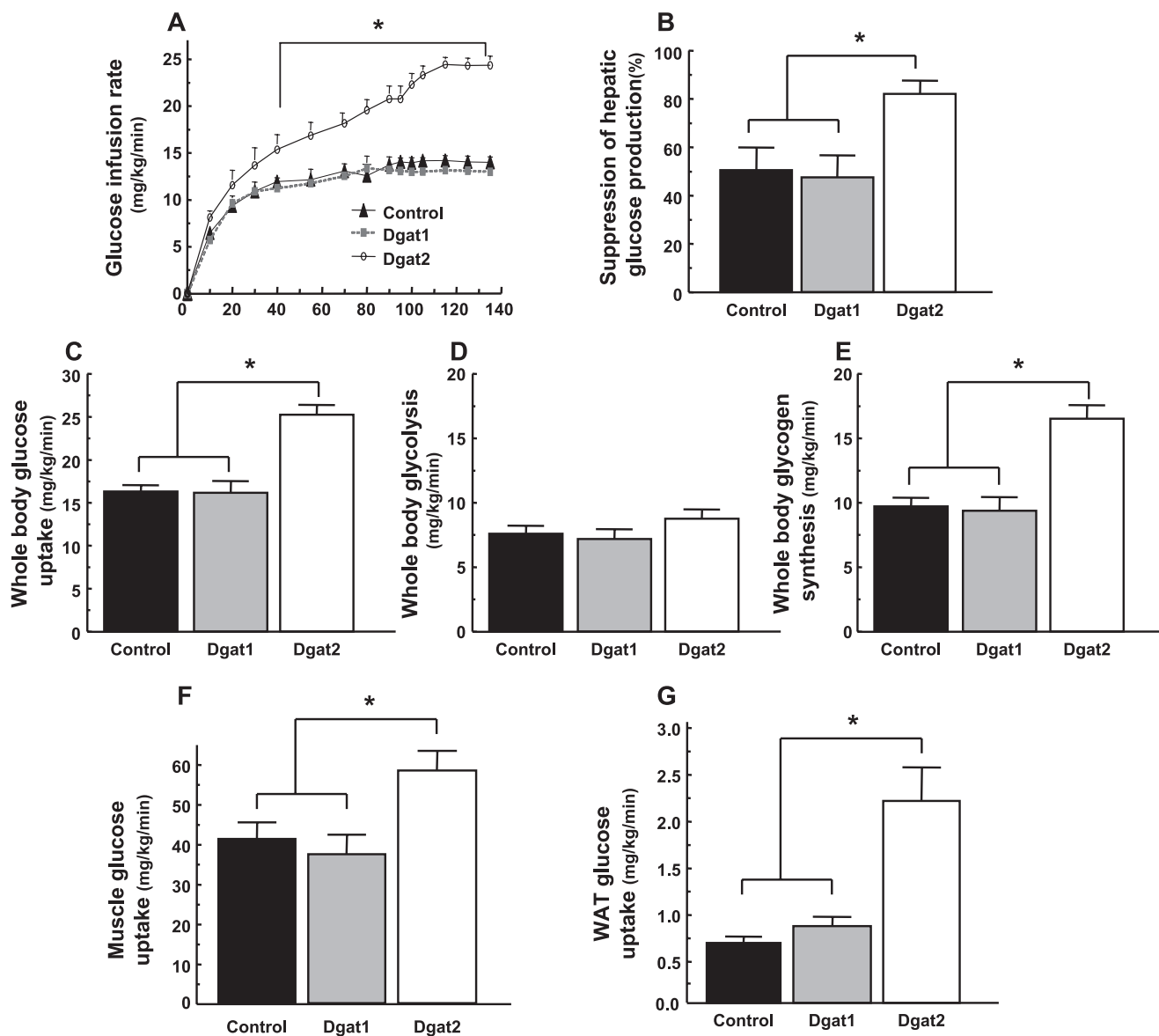


FIGURE 3. Dgat2 ASO treatment significantly improved hepatic and peripheral insulin sensitivity in high fat-fed rats. Peripheral and hepatic insulin sensitivities were assessed by means of hyperinsulinemic-euglycemic clamps. *A*, glucose infusion rates; *B*, suppression of hepatic glucose production (HGP) during hyperinsulinemic-euglycemic clamps; *C*, peripheral glucose disposal (Rd); *D*, whole body glycolysis; *E*, whole body glycogen synthesis; *F*, skeletal muscle (gastrocnemius) glucose uptake; and *G*, epididymal white adipose tissue (WAT) glucose uptake. Data are expressed as mean values \pm S.E. for 9–11 rats per treatment group; error bars indicate S.E. *, $p < 0.05$ versus ASOctrl and Dgat1 ASO treatment groups.

in Dgat2 ASO-treated rats, but adiponectin levels were unchanged. To independently assess hepatic and peripheral (predominantly muscle) insulin sensitivity, we performed hyperinsulinemic-euglycemic clamps (including radioisotope labeled glucose infusions) in ASO-treated rats. Glucose infusion rates were significantly higher in Dgat2 ASO but not in Dgat1 ASO-treated high fat fed rats than in the ASOctrl group (Fig. 3*A*). The ability of insulin to suppress endogenous glucose production was significantly increased in the Dgat2 ASO group (Fig. 3*B*) as was insulin-stimulated peripheral glucose turnover (47% increase, see Fig. 3*C*). Dgat2 ASO treatment did not change whole body glycolysis (Fig. 3*D*) but significantly increased glycogen synthesis rates by 71% as compared with ASOctrl therapy (Fig. 3*E*). The increase in insulin-stimulated glucose uptake was predominantly accounted for by a 35 and

230% increase in insulin-stimulated glucose uptake in skeletal muscle (gastrocnemius) and white adipose tissue (epididymal) (Fig. 3, *F* and *G*). The ability of insulin to suppress peripheral lipolysis and decrease fatty acid concentration also serves as an indicator of adipose tissue insulin sensitivity. In comparison with the control and Dgat1 ASO groups, Dgat2 ASO treatment increased insulin-mediated suppression of lipolysis, demonstrated by significantly lower fatty acid levels during the clamp (Table 1).

Effect of Dgat2 ASO Treatment on Hepatic Insulin Signaling—We have previously shown that hepatic steatosis (6) in rats fed a high fat diet for 3 days is specifically associated with activation of PKC ϵ (as reflected by an increase in the plasma membrane: cytosol ratio of PKC ϵ), an event that we believe may be causally related to the development of hepatic insulin resistance. Dgat2

Suppressing DGAT2 Reverses Hepatic Insulin Resistance

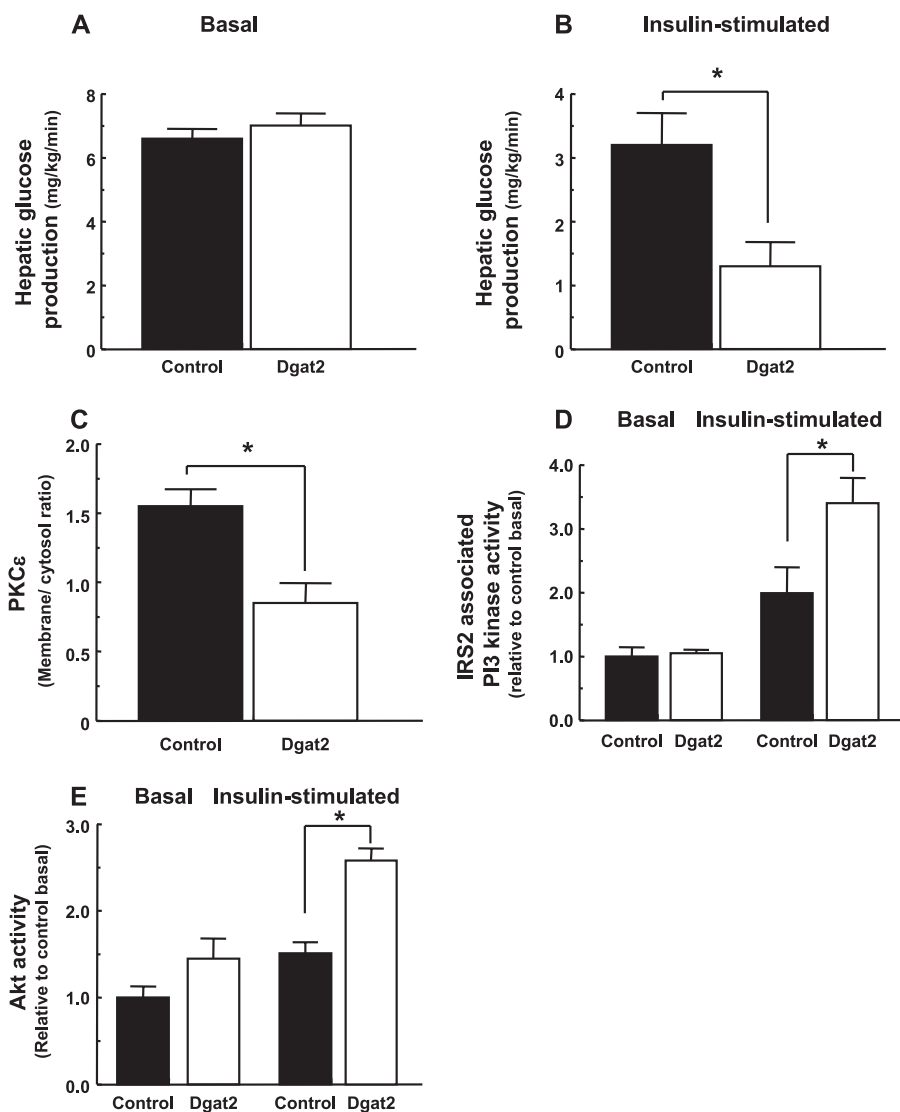


FIGURE 4. Dgat2 ASO treatment does not alter basal hepatic glucose production (A) but enhances insulin-mediated suppression of hepatic glucose production in high fat fed rats (B). Reduced PKC ϵ membrane translocation (C) may be directly involved in improving hepatic insulin signaling. This change is associated with increased IRS2-associated PI3K (D) and Akt2 activity (E). PI3K and Akt2 activity were assessed before (basal) and 20 min after primed infusion of insulin for PI3K in control (ASOctrl) and Dgat2 ASO-treated rats. Data are expressed as mean values \pm S.E. for 4 rats per treatment group; error bars indicate S.E. *, $p < 0.05$ versus ASOctrl treatment group.

ASO therapy significantly reduced hepatic glucose production during the hyperinsulinemic phase of the hyperinsulinemic-euglycemic clamp (Fig. 4, A and B) and significantly reduced PKC ϵ membrane translocation (Fig. 4C). These changes were associated with increased insulin-stimulated PI3K (Fig. 4D) and Akt2 activity (Fig. 4E).

Why Don't DAG Levels Increase in Dgat2 ASO-treated Rats?—As shown in Fig. 2, 4 weeks of Dgat2 ASO therapy significantly reduced liver DAGs and TGs, whereas liver LCCoAs were unchanged. To better understand this paradoxical observation, concentrations of plasma fatty acids and hepatic lipid intermediates in the TG synthesis pathway were measured at an early time point (3 days) after initiation of ASO therapy (Fig. 5). It is important to note that although maximum target gene suppression requires several doses of the antisense oligonucleotides, *DGAT2* mRNA was significantly reduced within 3 days of com-

mencing ASO therapy (Fig. 5A). At this stage, plasma fatty acids (Fig. 5B) were significantly increased, and hepatic LCCoAs tended to be increased ($p = 0.11$) (Fig. 5C), whereas LPA (Fig. 5D) and DAG levels (Fig. 5E) were similar to those in control rats. This metabolite pattern is similar to that observed in *mtGPAT* knock-out mice (12). Gene expression analysis confirmed that *mtGPAT* mRNA expression was reduced (Fig. 6A). This may in turn be due to the fatty acid-induced inhibition of sterol regulatory element-binding protein-1c (*Srebp1c*) activity (42, 43). *SREBP1c* mRNA and protein levels were also reduced at early time points as were levels of other lipogenic *SREBP1c* target genes, stearoyl-CoA desaturase-1 (*SCD1*) and *ACCI* (acetyl-CoA carboxylase 1) (Fig. 6, A and D). Importantly, plasma insulin levels were similar in Dgat2 and control ASO-treated rats at early time points (ASOctrl versus Dgat2 ASO; 6.0 ± 1.07 versus 4.4 ± 0.68 microunits/liter), so we do not believe that insulin was responsible for the early changes in lipogenic gene expression. Further evidence favoring increase in intracellular fatty acid rather than insulin as the signaling mediator of early changes in hepatic gene expression in this model comes from the fact that fatty acids might also be expected to activate PPAR α and increase PPAR α target gene expression. In this regard, PPAR α mRNA levels were unchanged, but *CPT1* mRNA and *UCP2* (uncoupling protein 2) mRNA and protein levels were increased, as were plasma ketones (2.23 ± 0.12 mmol/liter versus 1.92 ± 0.06 mmol/liter in control rats), an indirect marker of hepatic fatty acid oxidation (Fig. 6, B–D).

DISCUSSION

Hepatic steatosis is consistently associated with the development of hepatic insulin resistance in both rodent models and humans. Fat accumulation in the liver can occur as a result of increased fat delivery, increased fat synthesis, reduced fat oxidation, and/or reduced fat export in the form of lipoproteins (23). In humans, we have shown that reducing energy intake in association with modest weight loss reduces hepatic steatosis and improves hepatic insulin sensitivity in patients with T2DM (10). Unfortunately, lifestyle modification is notoriously difficult to sustain, necessitating the

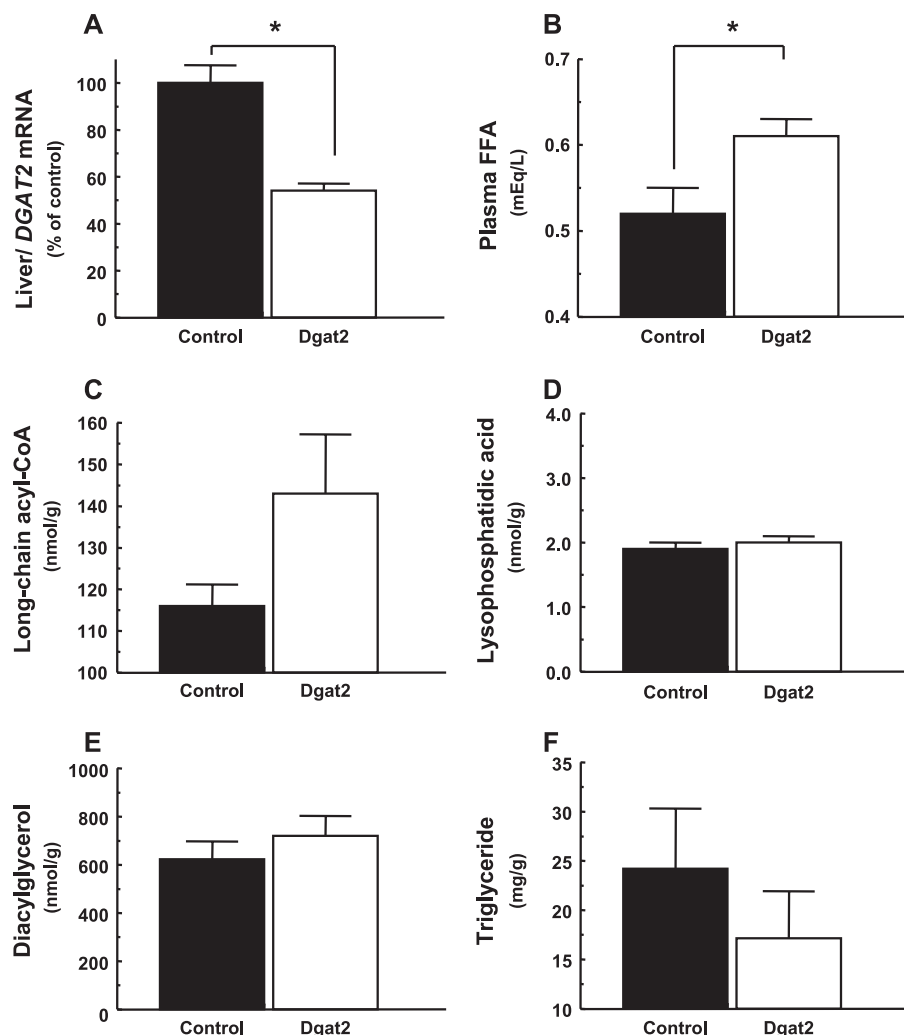


FIGURE 5. **Early effects of Dgat2 ASO therapy.** Within 3 days of commencing ASO therapy, *Dgat2* mRNA levels were significantly reduced (A). At this stage, plasma FFAs (B) were higher in Dgat2-treated rats, whereas hepatic LCCoAs (C), LPA (D), and DAG (E) levels were unchanged. Hepatic triglycerides (F) were already tending to be lower in Dgat2 ASO-treated rats. Data are expressed as mean values \pm S.E. for 6–8 rats per treatment group; error bars indicate S.E. *, $p < 0.05$ versus ASOctrl treatment group.

development of additional strategies for the treatment of NAFLD and hepatic insulin resistance. To date, the majority of studies has targeted fat oxidation with few attempts to reduce fat synthesis in the liver. Here we assessed the impact of antisense oligonucleotide-mediated reduction of Dgat1 or Dgat2 in rats with diet-induced NAFLD, an intervention that primarily influences TG synthesis. The results show that *DGAT1* and *DGAT2* were significantly reduced in an isoform- and tissue-selective (liver and adipose tissue) manner, and that there was no compensatory increase in the untargeted isoform. *DGAT1* knockdown was surprisingly ineffective in improving NAFLD in this model, whereas reducing *DGAT2* expression significantly improved hepatic steatosis. Although *DGAT1* null mice are resistant to diet-induced obesity and insulin resistance, this phenotype is dominated by an as yet incompletely understood increase in energy expenditure and weight loss (44). Interestingly, when adipose tissue was transplanted from *DGAT1* null mice to wild type mice, the latter lost weight, leading the authors to postulate that *DGAT1* knock-out adipocytes produce a circulating factor that promotes energy expenditure

(45). Recent work by the same group suggests that this putative factor is not adiponectin (46). Adiponectin levels were similar in all of our treatment groups. Our model differs from whole body knock-out studies in so far as *DGAT1* or *DGAT2* were selectively reduced in liver and adipose tissue (antisense oligonucleotides also reduce target gene expression in the kidney tubules but have no effect on muscle, bowel, or skin). The Dgat1 ASO does, however, reduce *DGAT1* expression in adipose tissue without significantly altering body weight. We did see a small reduction in weight gain in the Dgat2 ASO-treated group, a finding that we believe results from a small increase in energy expenditure as food intake and intestinal fat absorption were similar in ASOctrl and Dgat2 ASO-treated rats. The *DGAT2* null mouse is almost totally devoid of fat and dies shortly after birth, suggesting that Dgat2 may be more critical to TG synthesis than Dgat1 (20). This is in keeping with our data and with the reported efficacy of a Dgat2 ASO in mice with fatty liver (27). Dgat2 is also the predominant Dgat isoform in the liver (17) with almost no expression in stellate cells in mouse liver, whereas the expression of *DGAT1* is about 1.6-fold higher in stellate cells than in hepatocytes.⁶ These findings may help explain the lack of effect

of the Dgat1 ASO on hepatic triglyceride content.

Although ectopic fat accumulation in tissues such as liver and skeletal muscle is clearly associated with the development of insulin resistance, previous studies by our group have dissociated increase in intracellular TG from insulin resistance in skeletal muscle (15, 23). Early studies (3, 5, 47, 48) seemed to suggest that LCCoAs might be directly responsible for insulin resistance. However, few models have selectively altered LCCoAs without modifying DAG. In the *mtGPAT* null mouse liver, LCCoAs were significantly increased, whereas DAG and TG contents were reduced, and hepatic insulin sensitivity was improved, thereby dissociating elevated LCCoAs and insulin resistance (12). Intriguingly, Dgat2 knockdown also lowered liver DAG and TG content and improved hepatic insulin sensitivity despite similar hepatic LCCoA content compared with ASOctrl. The failure of intrahepatocellular DAG, a Dgat substrate, to increase following treatment with the Dgat2 ASO was

⁶ X. X. Yu, S. K. Pandey, J. G. Geisler, S. Bhanot, and B. P. Monia, unpublished observations.

Suppressing DGAT2 Reverses Hepatic Insulin Resistance

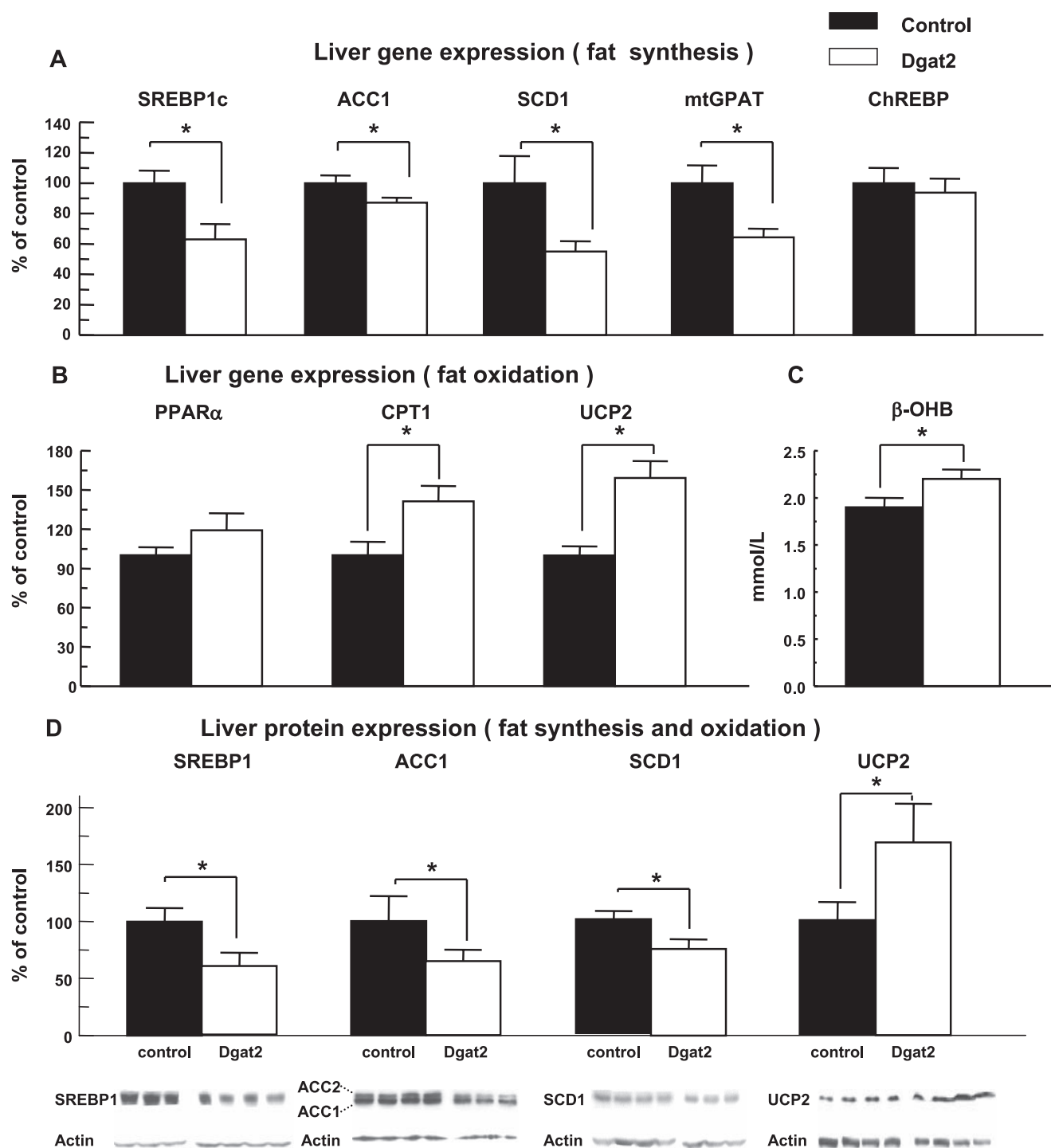


FIGURE 6. Early effects of Dgat2 ASO therapy on hepatic gene expression and ketone production. mRNA expression levels of genes involved in fat synthesis (A) and fat oxidation (B) were measured with real time RT-PCR. β -Hydroxybutyrate (ketone; β -OHB) levels were measured in fasting plasma samples (C). D, immunoblot analysis from selected genes as follows: fat synthesis (SREBP1, ACC1 and SCD1) and fat oxidation (UCP2). Data are expressed as mean values \pm S.E. for 6–8 rats per treatment group; error bars indicate S.E. *, $p < 0.05$ versus ASOctrl treatment group. ChREBP, carbohydrate-response element-binding protein; mtGPAT, mitochondrial acyl-CoA:glycerol-*sn*-3-phosphate acyltransferase; ACC1, acetyl-coenzyme A carboxylase 1; UCP2, uncoupling protein 2.

somewhat paradoxical and led to additional studies focused on elucidating the mechanism underlying this observation. Gene and protein expression analysis suggested that the lipogenic pathway was inhibited shortly after commencing Dgat2 ASO therapy. Fatty acids are well known to inhibit Srebp1c activity and expression (42, 43) and can also reduce transcriptional acti-

vation of lipogenic target genes by carbohydrate-response element-binding protein (49). The fact that mtGPAT mRNA expression was reduced in Dgat2 ASO-treated rats might explain, at least in part, the absence of an increase in LPA, DAG, and TG in the presence of increased plasma fatty acids, which are thought to be freely transported into the liver, and is con-

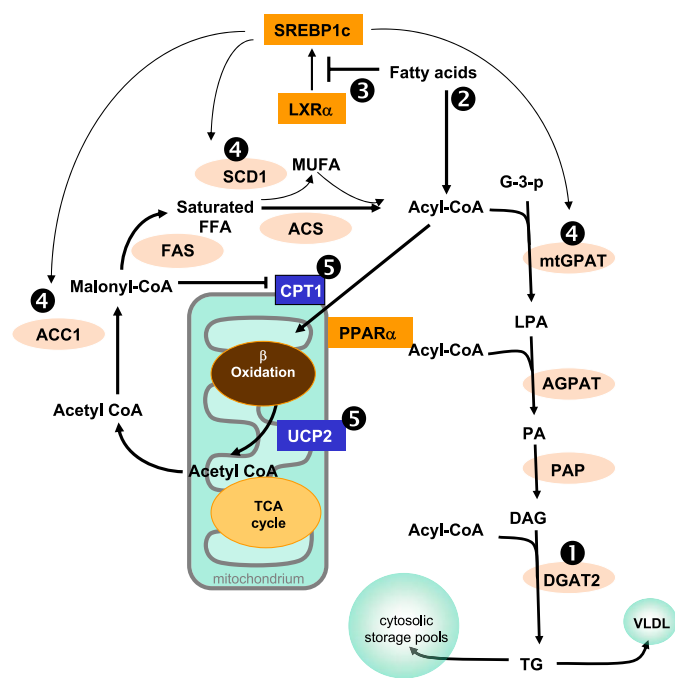


FIGURE 7. Schematic illustration of key elements of the triglyceride synthesis pathway and their modulation following Dgat 2 ASO therapy. Initially knocking down Dgat2 (step 1) increases plasma (and liver) fatty acids at early time points (step 2). As fatty acids, especially polyunsaturated fatty acids (PUFAs), are well known to inhibit liver X receptor α -mediated expression of SREBP1c (step 3), expression of SREBP1c and its target genes, mtGPAT, SCD1, and ACC1 was decreased (step 4), leading to reduced DAG content. Fatty acid accumulation also promotes fat oxidation by activating PPAR α , a key transcriptional regulator of hepatic fat oxidation, CPT1, and UCP2 in rodents (5). This potentially accounts for the observed increase in genes involved in fat oxidation and the early increase in plasma ketones. PA, phosphatidic acid; LPA, lysophosphatidic acid; acyl-CoA, long chain acyl CoA; PUFAs, polyunsaturated fatty acids; MUFAs, monounsaturated fatty acids; GPAT, acyl-CoA: glycerol-*sn*-3-phosphate acyltransferase; AGPAT, acyl-CoA:1-acylglycerol-*sn*-3-phosphate acyltransferase; PAP, phosphatidic acid phosphatase; DGAT2, acyl-CoA: diacylglycerol acyltransferase 2; LXR α , liver X receptor α ; ChREBP, carbohydrate-response element-binding protein, SCD1, stearoyl-CoA desaturase; ACC1, acetyl-coenzyme A carboxylase 1; CPT1, carnitine palmitoyl transferase 1; UCP2, uncoupling protein 2.

sistent with our findings in *mtGPAT* null mice. Fatty acid accumulation also promotes fat oxidation by activating PPAR α , a key transcriptional regulator of hepatic fat oxidation in rodents. Taken together, we believe that the reason DAG does not accumulate and induce hepatic insulin resistance in Dgat2 ASO-treated animals is at least in part attributable to activation of compensatory pathways in response to increased hepatocellular fatty acid content. One compensatory pathway might involve polyunsaturated fatty acid (PUFA) suppression of the lipogenic pathway by inhibiting Srebp1c expression and activity, as reflected by reduced Srebp1c target gene and protein expression (Fig. 7). Exactly how PUFAs suppress Srebp1c activity remains to be determined, but suggested mechanisms include interference with liver X receptor activity at the promoter of SREBP1c (43), effects on Srebp1c maturation, and possibly even effects on another key lipogenic regulator, carbohydrate-response element-binding protein (49). Fatty acids are also known to activate PPAR α (50), potentially accounting for the observed increase in genes involved in fat oxidation, the early increase in plasma ketones, and weight loss. As Dgat ASO therapy had no effect on Dgat expression in skeletal muscle, we

believe that the improvement in insulin-stimulated peripheral glucose turnover is a consequence of reduced body weight and lower intramuscular lipid content.

This study provides further support for the hypothesis that PKC ϵ activation may be causally implicated in hepatic lipid-induced insulin resistance as Dgat2 knockdown led to a significant decrease in DAG content and PKC ϵ activation in association with improvements in insulin signaling and *in vivo* hepatic insulin sensitivity. PKC ϵ activation has now been linked to fatty liver and hepatic insulin resistance in several rodent models (6, 12) and in humans (13). We have also recently shown that reducing hepatic PKC ϵ expression in the liver of high fat-fed rats prevents the development of hepatic insulin resistance (11). Co-immunoprecipitation studies suggest that PKC ϵ binds to the insulin receptor and inhibits its tyrosine kinase activity (11).

In summary, our study suggests that in this rat model of diet-induced NAFLD, targeting Dgat2, but not Dgat1, with antisense oligonucleotides successfully improves hepatic steatosis, hepatic insulin signaling, and *in vivo* hepatic insulin sensitivity. We also proposed a novel explanation for the paradoxical decrease in diacylglycerol concentrations in Dgat2 ASO-treated rats and provided further support for the notion that diacylglycerol accumulation and PKC ϵ activation cause insulin resistance in NAFLD. It will be of great interest to see if alternative strategies for lowering hepatic diacylglycerol levels yield similar therapeutic results in patients with NAFLD and T2DM.

Acknowledgments—We thank Jianying Dong and Richard Lee for expert technical assistance with the studies and Aida Groszmann for performing the hormone assays.

REFERENCES

- Browning, J. D., and Horton, J. D. (2004) *J. Clin. Investig.* **114**, 147–152
- Browning, J. D., Szczepaniak, L. S., Dobbins, R., Nuremberg, P., Horton, J. D., Cohen, J. C., Grundy, S. M., and Hobbs, H. H. (2004) *Hepatology* **40**, 1387–1395
- Kim, H. J., Lee, K. E., Kim, D. J., Kim, S. K., Ahn, C. W., Lim, S. K., Kim, K. R., Lee, H. C., Huh, K. B., and Cha, B. S. (2004) *Arch. Intern. Med.* **164**, 2169–2175
- Seppala-Lindroos, A., Vehkavaara, S., Hakkinen, A. M., Goto, T., Westerbacka, J., Sovijarvi, A., Halavaara, J., and Yki-Jarvinen, H. (2002) *J. Clin. Endocrinol. Metab.* **87**, 3023–3028
- Kim, J. K., Fillmore, J. J., Chen, Y., Yu, C., Moore, I. K., Pypaert, M., Lutz, E. P., Kako, Y., Velez-Carrasco, W., Goldberg, I. J., Breslow, J. L., and Shulman, G. I. (2001) *Proc. Natl. Acad. Sci. U. S. A.* **98**, 7522–7527
- Samuel, V. T., Liu, Z. X., Qu, X., Elder, B. D., Bilz, S., Befroy, D., Romanelli, A. J., and Shulman, G. I. (2004) *J. Biol. Chem.* **279**, 32345–32353
- Savage, D. B., Choi, C. S., Samuel, V. T., Liu, Z. X., Zhang, D., Wang, A., Zhang, X. M., Cline, G. W., Yu, X. X., Geisler, J. G., Bhanot, S., Monia, B. P., and Shulman, G. I. (2006) *J. Clin. Investig.* **116**, 817–824
- An, J., Muoio, D. M., Shiota, M., Fujimoto, Y., Cline, G. W., Shulman, G. I., Koves, T. R., Stevens, R., Millington, D., and Newgard, C. B. (2004) *Nat. Med.* **10**, 268–274
- Ishigaki, Y., Katagiri, H., Yamada, T., Ogihara, T., Imai, J., Uno, K., Hasegawa, Y., Gao, J., Ishihara, H., Shimosegawa, T., Sakoda, H., Asano, T., and Oka, Y. (2005) *Diabetes* **54**, 322–332
- Petersen, K. F., Dufour, S., Befroy, D., Lehrke, M., Hendler, R. E., and Shulman, G. I. (2005) *Diabetes* **54**, 603–608
- Samuel, V. T., Liu, Z. X., Wang, A., Beddow, S. A., Geisler, J. G., Kahn, M., Zhang, X. M., Monia, B. P., Bhanot, S., and Shulman, G. I. (2007) *J. Clin.*

Suppressing DGAT2 Reverses Hepatic Insulin Resistance

- Investig.* **117**, 737–745
12. Neschen, S., Morino, K., Hammond, L. E., Zhang, D., Liu, Z. X., Romanelli, A. J., Cline, G. W., Pongratz, R. L., Zhang, X. M., Choi, C. S., Coleman, R. A., and Shulman, G. I. (2005) *Cell Metab.* **2**, 55–65
 13. Considine, R. V., Nyce, M. R., Allen, L. E., Morales, L. M., Triester, S., Serrano, J., Colberg, J., Lanza-Jacoby, S., and Caro, J. F. (1995) *J. Clin. Investig.* **95**, 2938–2944
 14. Shmueli, E., Alberti, K. G., and Record, C. O. (1993) *J. Intern. Med.* **234**, 397–400
 15. Yu, C., Chen, Y., Cline, G. W., Zhang, D., Zong, H., Wang, Y., Bergeron, R., Kim, J. K., Cushman, S. W., Cooney, G. J., Atcheson, B., White, M. F., Kraegen, E. W., and Shulman, G. I. (2002) *J. Biol. Chem.* **277**, 50230–50236
 16. Cases, S., Smith, S. J., Zheng, Y. W., Myers, H. M., Lear, S. R., Sande, E., Novak, S., Collins, C., Welch, C. B., Lusis, A. J., Erickson, S. K., and Farese, R. V., Jr. (1998) *Proc. Natl. Acad. Sci. U. S. A.* **95**, 13018–13023
 17. Cases, S., Stone, S. J., Zhou, P., Yen, E., Tow, B., Lardizabal, K. D., Voelker, T., and Farese, R. V., Jr. (2001) *J. Biol. Chem.* **276**, 38870–38876
 18. Chen, H. C., Smith, S. J., Ladha, Z., Jensen, D. R., Ferreira, L. D., Pulawa, L. K., McGuire, J. G., Pitas, R. E., Eckel, R. H., and Farese, R. V., Jr. (2002) *J. Clin. Investig.* **109**, 1049–1055
 19. Smith, S. J., Cases, S., Jensen, D. R., Chen, H. C., Sande, E., Tow, B., Sanan, D. A., Raber, J., Eckel, R. H., and Farese, R. V., Jr. (2000) *Nat. Genet.* **25**, 87–90
 20. Stone, S. J., Myers, H. M., Watkins, S. M., Brown, B. E., Feingold, K. R., Elias, P. M., and Farese, R. V., Jr. (2004) *J. Biol. Chem.* **279**, 11767–11776
 21. Petersen, K. F., and Shulman, G. I. (2006) *Am. J. Med.* **119**, S10–S16
 22. Reznick, R. M., and Shulman, G. I. (2006) *J. Physiol. (Lond.)* **574**, 33–39
 23. Shulman, G. I. (2000) *J. Clin. Investig.* **106**, 171–176
 24. Watts, L. M., Mancham, V. P., Leedom, T. A., Rivard, A. L., McKay, R. A., Bao, D., Neroladakis, T., Monia, B. P., Bodenmiller, D. M., Cao, J. X., Zhang, H. Y., Cox, A. L., Jacobs, S. J., Michael, M. D., Sloop, K. W., and Bhanot, S. (2005) *Diabetes* **54**, 1846–1853
 25. McKay, R. A., Miraglia, L. J., Cummins, L. L., Owens, S. R., Sasmor, H., and Dean, N. M. (1999) *J. Biol. Chem.* **274**, 1715–1722
 26. Lehner, R., and Kuksis, A. (1993) *J. Biol. Chem.* **268**, 8781–8786
 27. Yu, X. X., Murray, S. F., Pandey, S. K., Booten, S. L., Bao, D., Song, X. Z., Kelly, S., Chen, S., McKay, R., Monia, B. P., and Bhanot, S. (2005) *Hepatology* **42**, 362–371
 28. Crooke, R. M., Graham, M. J., Lemonidis, K. M., Whipple, C. P., Koo, S., and Perera, R. J. (2005) *J. Lipid Res.* **46**, 872–884
 29. Youn, J. H., and Buchanan, T. A. (1993) *Diabetes* **42**, 757–763
 30. Rossetti, L., and Giaccari, A. (1990) *J. Clin. Investig.* **85**, 1785–1792
 31. Ohshima, K., Shargill, N. S., Chan, T. M., and Bray, G. A. (1984) *Am. J. Physiol.* **246**, E193–E197
 32. Bligh, E. G., and Dyer, W. J. (1959) *Can. J. Biochem. Physiol.* **37**, 911–917
 33. Neschen, S., Moore, I., Regittign, W., Yu, C. L., Wang, Y., Pypaert, M., Petersen, K. F., and Shulman, G. I. (2002) *Am. J. Physiol.* **282**, E395–E401
 34. Alessi, D. R., Andjelkovic, M., Caudwell, B., Cron, P., Morrice, N., Cohen, P., and Hemmings, B. A. (1996) *EMBO J.* **15**, 6541–6551
 35. Folli, F., Saad, M. J., Backer, J. M., and Kahn, C. R. (1992) *J. Biol. Chem.* **267**, 22171–22177
 36. Qu, X., Seale, J. P., and Donnelly, R. (1999) *J. Endocrinol.* **162**, 207–214
 37. Jandacek, R. J., Heubi, J. E., and Tso, P. (2004) *Gastroenterology* **127**, 139–144
 38. Cao, J., Lockwood, J., Burn, P., and Shi, Y. (2003) *J. Biol. Chem.* **278**, 13860–13866
 39. Cao, J., Cheng, L., and Shi, Y. (2007) *J. Lipid Res.* **48**, 583–591
 40. Coleman, R. A., and Lee, D. P. (2004) *Prog. Lipid Res.* **43**, 134–176
 41. Yen, C. L., and Farese, R. V., Jr. (2003) *J. Biol. Chem.* **278**, 18532–18537
 42. Jump, D. B., Clarke, S. D., Thelen, A., and Liimatta, M. (1994) *J. Lipid Res.* **35**, 1076–1084
 43. Ou, J., Tu, H., Shan, B., Luk, A., DeBose-Boyd, R. A., Bashmakov, Y., Goldstein, J. L., and Brown, M. S. (2001) *Proc. Natl. Acad. Sci. U. S. A.* **98**, 6027–6032
 44. Chen, H. C., and Farese, R. V., Jr. (2005) *Arterioscler. Thromb. Vasc. Biol.* **25**, 482–486
 45. Chen, H. C., Jensen, D. R., Myers, H. M., Eckel, R. H., and Farese, R. V., Jr. (2003) *J. Clin. Investig.* **111**, 1715–1722
 46. Streeper, R. S., Koliwad, S. K., Villanueva, C. J., and Farese, R. V., Jr. (2006) *Am. J. Physiol.* **291**, E388–E394
 47. Kim, J. K., Gimeno, R. E., Higashimori, T., Kim, H. J., Choi, H., Punreddy, S., Mozell, R. L., Tan, G., Stricker-Krongrad, A., Hirsch, D. J., Fillmore, J. J., Liu, Z. X., Dong, J., Cline, G., Stahl, A., Lodish, H. F., and Shulman, G. I. (2004) *J. Clin. Investig.* **113**, 756–763
 48. Cooney, G. J., Thompson, A. L., Furler, S. M., Ye, J., and Kraegen, E. W. (2002) *Ann. N. Y. Acad. Sci.* **967**, 196–207
 49. Dentin, R., Benhamed, F., Pegorier, J. P., Fougelle, F., Viollet, B., Vaulont, S., Girard, J., and Postic, C. (2005) *J. Clin. Investig.* **115**, 2843–2854
 50. Jump, D. B., Botolin, D., Wang, Y., Xu, J., Christian, B., and Demeure, O. (2005) *J. Nutr.* **135**, 2503–2506

Suppression of Diacylglycerol Acyltransferase-2 (*DGAT2*), but Not *DGAT1*, with Antisense Oligonucleotides Reverses Diet-induced Hepatic Steatosis and Insulin Resistance

Cheol Soo Choi, David B. Savage, Ameya Kulkarni, Xing Xian Yu, Zhen-Xiang Liu, Katsutaro Morino, Sheene Kim, Alberto Distefano, Varman T. Samuel, Susanne Neschen, Dongyan Zhang, Amy Wang, Xian-Man Zhang, Mario Kahn, Gary W. Cline, Sanjay K. Pandey, John G. Geisler, Sanjay Bhanot, Brett P. Monia and Gerald I. Shulman

J. Biol. Chem. 2007, 282:22678-22688.

doi: 10.1074/jbc.M704213200 originally published online May 27, 2007

Access the most updated version of this article at doi: [10.1074/jbc.M704213200](https://doi.org/10.1074/jbc.M704213200)

Alerts:

- [When this article is cited](#)
- [When a correction for this article is posted](#)

[Click here](#) to choose from all of JBC's e-mail alerts

This article cites 50 references, 22 of which can be accessed free at <http://www.jbc.org/content/282/31/22678.full.html#ref-list-1>